



This is a repository copy of *Deficiency in the mRNA export mediator Gle1 impairs Schwann cell development in the zebrafish embryo.*

White Rose Research Online URL for this paper:
<http://eprints.whiterose.ac.uk/96828/>

Version: Accepted Version

Article:

Alsomali, N., Seytanoglu, A., Valori, C. et al. (6 more authors) (2016) Deficiency in the mRNA export mediator Gle1 impairs Schwann cell development in the zebrafish embryo. *Neuroscience*, 322. pp. 287-297. ISSN 0306-4522

<https://doi.org/10.1016/j.neuroscience.2016.02.039>

Article available under the terms of the CC-BY-NC-ND licence
(<https://creativecommons.org/licenses/by-nc-nd/4.0/>)

Reuse

This article is distributed under the terms of the Creative Commons Attribution-NonCommercial-NoDerivs (CC BY-NC-ND) licence. This licence only allows you to download this work and share it with others as long as you credit the authors, but you can't change the article in any way or use it commercially. More information and the full terms of the licence here: <https://creativecommons.org/licenses/>

Takedown

If you consider content in White Rose Research Online to be in breach of UK law, please notify us by emailing eprints@whiterose.ac.uk including the URL of the record and the reason for the withdrawal request.



eprints@whiterose.ac.uk
<https://eprints.whiterose.ac.uk/>

Accepted Manuscript

Deficiency in the mRNA export mediator Gle1 impairs Schwann cell development in the zebrafish embryo

Adil Seytanoglu, Nimah I. Alsomali, Chiara F. Valori, Alexander McGown, H. Rosemary Kim, Ke Ning, Tennore Ramesh, Basil Sharrack, Jonathan D. Wood, Mimoun Azzouz

PII: S0306-4522(16)00179-2

DOI: <http://dx.doi.org/10.1016/j.neuroscience.2016.02.039>

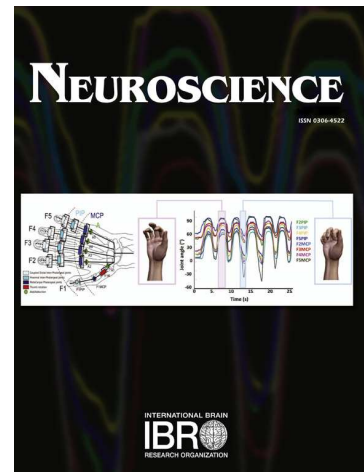
Reference: NSC 16929

To appear in: *Neuroscience*

Accepted Date: 17 February 2016

Please cite this article as: A. Seytanoglu, N.I. Alsomali, C.F. Valori, A. McGown, H.R. Kim, K. Ning, T. Ramesh, B. Sharrack, J.D. Wood, M. Azzouz, Deficiency in the mRNA export mediator Gle1 impairs Schwann cell development in the zebrafish embryo, *Neuroscience* (2016), doi: <http://dx.doi.org/10.1016/j.neuroscience.2016.02.039>

This is a PDF file of an unedited manuscript that has been accepted for publication. As a service to our customers we are providing this early version of the manuscript. The manuscript will undergo copyediting, typesetting, and review of the resulting proof before it is published in its final form. Please note that during the production process errors may be discovered which could affect the content, and all legal disclaimers that apply to the journal pertain.



Deficiency in the mRNA export mediator Gle1 impairs Schwann cell development in the zebrafish embryo

Adil Seytanoglu^{1,*}, Nimah I. Alsomali^{1,*,\$}, Chiara F. Valori^{1,†}, Alexander McGown¹, H.

Rosemary Kim², Ke Ning¹, Tennore Ramesh¹, Basil Sharrack^{1,3}, Jonathan D. Wood^{1,2,**},

Mimoun Azzouz^{1,4,**,#}

¹The Sheffield Institute for Translational Neuroscience, Department of Neuroscience, University of Sheffield, 385A Glossop Road, Sheffield, S10 2HQ, UK.

²Bateson Centre, Department of Biomedical Science, University of Sheffield, Firth Court, Western Bank, Sheffield, S10 2TN, UK

³Department of Neurology, Royal Hallamshire Hospital, Sheffield Teaching Hospitals Foundation Trust, Glossop Road, Sheffield, S10 2JF, UK.

⁴Faculty of Medicine, King Abdulaziz University, Jeddah, Saudi Arabia

†Present Address: German Centre for Neurodegenerative Diseases (DZNE) c/o TTR Paul-Ehrlich-Str. 1772076 Tübingen, Germany

\$Present address: National Neuroscience Institute, King Fahad Medical City, Riyadh, Saudi Arabia

*Joint first authors

** Equal contribution to the work

Correspondence should be addressed to:

Mimoun Azzouz, The Sheffield Institute for Translational Neuroscience, University of Sheffield, 385A Glossop Road, Sheffield, S10 2HQ, UK.

Tel: 0044 (0)114 222238

E-mail: m.azzouz@sheffield.ac.uk

Abstract - *GLE1* mutations cause lethal congenital contracture syndrome 1 (LCCS1), a severe autosomal recessive fetal motor neuron disease, and more recently have been associated with amyotrophic lateral sclerosis (ALS). The gene encodes a highly conserved protein with an essential role in mRNA export. The mechanism linking Gle1 function to motor neuron degeneration in humans has not been elucidated, but increasing evidence implicates abnormal RNA processing as a key event in the pathogenesis of several motor neuron diseases. Homozygous *gle1*^{-/-} mutant zebrafish display various aspects of LCCS, showing severe developmental abnormalities including motor neuron arborisation defects and embryonic lethality. A previous gene expression study on spinal cord from LCCS fetuses indicated that oligodendrocyte dysfunction may be an important factor in LCCS. We therefore set out to investigate the development of myelinating glia in *gle1*^{-/-} mutant zebrafish embryos. While expression of *myelin basic protein (mbp)* in hindbrain oligodendrocytes appeared relatively normal, our studies revealed a prominent defect in Schwann cell precursor proliferation and differentiation in the posterior lateral line nerve. Other genes mutated in LCCS have important roles in Schwann cell development, thereby suggesting that Schwann cell deficits may be a common factor in LCCS pathogenesis. These findings illustrate the potential importance of glial cells such as myelinating Schwann cells in motor neuron diseases linked to RNA processing defects.

Keywords: Lethal congenital contracture syndrome 1; motor neuron; zebrafish model; Schwann cell development.

INTRODUCTION

Emerging evidence suggests that abnormal RNA processing is an important factor in motor neuron diseases, including amyotrophic lateral sclerosis (ALS), spinal muscular atrophy (SMA) and lethal congenital contracture syndrome I (LCCS1) (Ibrahim et al., 2012). Mutations in various RNA-binding proteins, such as SMN, TARDBP, FUS and GLE1 have been identified as genetic causes of motor neuron degeneration (Lefebvre et al., 1995, Sreedharan et al., 2008, Nousiainen et al., 2008, Vance et al., 2009). The *GLE1* gene is mutated in LCCS1, a severe autosomal recessive fetal motor neuron disease (Nousiainen et al., 2008). The disease is characterized by total immobility of the fetus, which can be detected around the 13th week of gestation (Nousiainen et al., 2008). Other symptoms include hypoplasia, pytergia, multiple joint contractures and micrognathia. Prenatal death usually occurs before the 32nd gestation week (Nousiainen et al., 2008). More recently, it has been suggested that haploinsufficiency for *GLE1* may be a genetic factor predisposing to ALS (Kaneb et al., 2015).

The *GLE1* gene is highly conserved between species (Alcazar-Roman et al., 2006, Bolger et al., 2008). In humans, it encodes two protein coding isoforms; GLE1A and GLE1B. The peptide sequences of GLE1A and GLE1B are highly similar. They differ in the C-terminal region where GLE1B has an additional, functionally important 43 amino acid domain (Kendirgi et al., 2003). This additional domain is necessary and sufficient for the interaction with CG1 (a nucleoporin, also known as NUPL2) (Kendirgi et al., 2003). *GLE1-002* mRNA, which produces the 698 amino acid GLE1B peptide, is reported to be expressed about a thousand times more than the *GLE1-001* mRNA encoding GLE1A in HeLa cells and its product dominates the intracellular localization profile (Kendirgi et al., 2003). The GLE1 protein has nuclear pore complex (NPC) targeting, coiled-coil, nuclear shuttling and nuclear rim targeting domains (Rayala et al., 2004, Kendirgi et al., 2005, Nousiainen et al., 2008). It

has been shown to have several essential roles in vital cellular processes such as mRNA export, translation initiation and translation termination.

Studies in *Saccharomyces cerevisiae* identified Gle1 (also known as RSS1) as an essential yeast RNA export protein involved in the Poly(A)⁺ RNA export (Murphy and Wente, 1996, Watkins et al., 1998). Additional studies in yeast showed that Gle1 has a crucial role in mRNA-protein (mRNP) complex remodeling. Inositol hexakisphosphate (IP₆)-bound Gle1 activates DEAD box protein 5 (Dbp5; DDX19 in humans) on the cytoplasmic face of the nuclear pore complex (NPC) (Alcazar-Roman et al., 2006) by stimulating ATP binding to Dbp5 (Noble et al., 2011). In return, Dbp5 mediates the dissociation of protein components from mRNPs (Tran et al., 2007, Hodge et al., 2011). It has been reported that Gle1 has other functionally distinct roles in translation. Studies in yeast suggest that it is involved in translation termination through IP₆-dependent Dbp5 activation, and in translation initiation in an IP₆/Dbp5-independent manner (Bolger et al., 2008).

Mutations in other genes have been found to cause LCCS. LCCS2 is caused by mutation of *ERBB3* (Narkis et al., 2007b), a member of the ERBB family of receptor tyrosine kinases; LCCS3 is caused by mutation of *PIP5K1C* (Narkis et al., 2007a), which encodes phosphatidylinositol-4-phosphate 5-kinase, type I, gamma (PIPKI γ); LCCS5 is caused by homozygous *Dynamin 2* (*DNM2*) mutation (Koutsopoulos et al., 2013); while another study linked mutations in *CNTNAP1* (encoding contactin associated protein 1) and *ADCY6* (encoding adenylate cyclase 6) to LCCS7 and LCCS8 respectively (Laqu rri re et al., 2014). These LCCS genes have all been associated with Schwann cell development or function. *ErbB3* was shown to be important for Schwann cell survival in the mouse (Riethmacher et al., 1997), while its orthologue *erbb3* was shown to be specifically required for migration and proliferation of Schwann cell precursors in the zebrafish embryo (Lyons et al., 2005). PIPKI γ phosphorylates phosphatidylinositol 4-phosphate to generate phosphatidylinositol-4,5-bisphosphate (PIP₂) and the localized synthesis of PIP₂ is important for asymmetric process retraction during directional Schwann cell migration (Gatto et al., 2007). Dynamin 2 is

involved in clathrin-mediated endocytosis and required for Schwann cell myelination (Sidiropoulos et al., 2012), CNTNAP1 is an essential component of Ranvier domains, while knockdown of ADCY6 orthologues in zebrafish blocked PNS myelination (Laquérière et al., 2014). GLE1 function has not been associated with PNS myelination, however RNA expression profiling of spinal cord from LCCS1 fetuses indicated that oligodendrocyte dysfunction may be a factor in disease pathogenesis (Pakkasjarvi et al., 2006).

The zebrafish has been extensively used as a model organism for neurodegenerative disorders (for review see (Kabashi et al., 2010, Xi et al., 2011)), including models of motor neuron diseases such as SMA (Boon et al., 2009) and ALS (Ramesh et al., 2010). A zebrafish model of LCCS1 has recently been reported, with *gle1*^{-/-} embryos showing multiple defects, including immobility, small eyes, pharyngeal arch defects, CNS cell death, a moderate reduction in motor neuron numbers and motor axon outgrowth defects (Jao et al., 2012). These modest motor neuron development defects are somewhat surprising given the marked loss of motor neurons reported in the spinal cord of LCCS1 fetuses, suggesting that additional factors may contribute to motor neuron survival in LCCS1. Given the known role of other LCCS genes in Schwann cell development and evidence for oligodendrocyte dysfunction in LCCS1 spinal cord, we therefore reasoned that *gle1* may be required for the development of myelinating glia in the zebrafish embryo. We herein demonstrate a novel critical requirement for *gle1*, and therefore mRNA export function, not only for motor neuron survival but also in Schwann cell development.

EXPERIMENTAL PROCEDURES

Zebrafish maintenance

All procedures involving animals were performed according to UK Home Office regulations and subjected to ethical review and approval by the Ethics Review Committee at the

University of Sheffield. *gle1*^{hi4161aTg/+} carriers (Amsterdam et al., 2004) were obtained from the Zebrafish International Resource Center (ZIRC), Oregon, USA and out-crossed on to a TL background. Carriers were identified by PCR using a forward primer that anneals to the 3' region of the retrovirus (5'-CGCTTCTCGCTTCTGTTCG-3') and a reverse primer (5'-GGCTGTATTTGAGTTTCCCCTTC-3') that anneals to the adjacent genomic region. The *Tg(sox10:mRFP)* line, which expresses mRFP in multiple neural crest-derived cell types, including Schwann cell precursors (Kucenas et al., 2008), was obtained from Dr. David Lyons (University of Edinburgh) with permission from Dr. Bruce Appel (University of Colorado Denver) and crossed with *gle1*^{hi4161aTg/+} carriers to facilitate detection of Schwann cell precursors. Embryos were obtained by natural mating.

Survival and motility assays

Embryos were raised in petri dishes containing E3 medium until 5 dpf. They were then moved to larger tanks containing aquarium water and fed daily. Dead embryos were collected twice daily and genotyped. A Kaplan-Meier survival plot was generated using Prism v5.04 software (Graphpad Software, USA). Motility of mutant and sibling embryos was quantified over a 2-hour period at 4, 5 and 6 dpf. Mutants and siblings (24 each) were sorted on morphological phenotypes and placed in individual wells of a 48-well plate. The plate was placed in the Zebrabox (Viewpoint Life Sciences, Lyon, France) viewing chamber at 28°C. The light cycle in the chamber was set for 25 minutes of dark followed by 5 minutes of light exposure. The motility of the embryos and the total distance covered by each embryo was recorded using Zebralab v3.20. The data were analysed with an unpaired *t* test using Graphpad Prism v5.04.

TUNEL staining

Embryos were anaesthetized in Tricaine and fixed in 4% PFA in PBS at 4°C overnight. After fixation they were briefly washed in water then incubated in pre-chilled acetone at -20°C for

7 minutes. They were then washed in PBS + 0.1% Tween 20 (PBT) and digested with 10 µg/ml Proteinase K (Sigma) in PBT. Samples were then washed with PBT and briefly fixed in 4% PFA in PBS at room temperature. TUNEL staining was performed using the ApopTag Red *in situ* apoptosis kit (Millipore). Following further PBT washes, samples were incubated in equilibration buffer for 1 hour at room temperature. Samples were then incubated in reaction buffer and TdT enzyme mix at 37°C for 90 minutes. This was then replaced with stop buffer and samples incubated at 37°C for 3 hours. They were then washed in PBT and incubated with a rhodamine-labeled anti-DIG antibody diluted in blocking solution overnight at 4°C. The samples were washed thoroughly in PBT, fixed in 4% PFA in PBS for 30 minutes and washed with PBT once more. They were moved through a series of glycerol dilutions to 75% glycerol/25% PBS and mounted for confocal microscopy. Samples were imaged using an Olympus Fluoview FV1000 confocal microscope.

H&E staining

Embryos were fixed overnight in 4% PFA. Sections were cut from paraffin-embedded specimens, floated on warm water, collected on slides and incubated at 42°C overnight. The next day, they were brought to room temperature and de-waxed in xylene for five minutes. After a second wash in xylene, they were washed twice with absolute ethanol and then rehydrated by briefly incubating consecutively in 95% and 70% ethanol. Samples were then transferred to Harris' haematoxylin solution (Leica, UK) for three minutes. They were rinsed in water and dipped in acid-alcohol solution before another wash in water, and then placed in Scott's solution for approximately fifteen seconds. Following a rinse, samples were incubated in eosin (Surgipath, UK) for five minutes. They were rinsed quickly in water and gradually moved to 100% ethanol. Samples were placed in fresh xylene and mounted in a hard set mounting medium (Vector Laboratories). Samples were viewed using a compound microscope.

Whole mount *in situ* hybridization and immunohistochemistry

In situ hybridization and immunohistochemistry were performed using standard protocols. Digoxigenin-labeled riboprobes were prepared from linearised plasmid templates with SP6 and T7 polymerases as recommended by the supplier (Roche Life Sciences). Staining was visualized using an anti-DIG-alkaline phosphatase conjugated antibody and NBT/BCIP (Roche Life Sciences). Monoclonal anti-acetylated tubulin clone 6-11B-1 (Sigma) was used at 1:5000 and staining visualized using VectaStain Elite ABC and DAB Peroxidase Substrate kits (Vector Laboratories).

EdU labeling and detection

Embryos were anaesthetized by immersion in Tricaine and injected directly into the yolk mass with 5 nl of 5 mM 5-ethynyl-2'-deoxyuridine (EdU) in 0.15x Danieau's solution at 52 hpf. They were then incubated at room temperature for 1 h to enable EdU incorporation prior to overnight fixation in 4% paraformaldehyde. Fixed embryos were stored in methanol for at least 24 hours, then rehydrated and permeabilised in acetone at -20°C for 10 min. EdU-labeled cells were detected using a Click-iT EdU Alexa Fluor 647 imaging kit (Life Technologies). mRFP was subsequently immunostained using a rabbit polyclonal anti-DsRed antibody (Clontech) and Alexa Fluor 488 goat anti-rabbit secondary antibody (Life Technologies). Fluorescence was visualized using a Leica TCS SP5 II confocal microscope. EdU-labelled cells were counted in 100 µm segments along the posterior lateral line nerve (PLLn) in 3 specimens per group. Graphpad Prism was used to calculate mean cell counts ± S.E.M. and statistical significance determined using a Mann-Whitney U test.

Transmission electron microscopy (TEM)

Transmission electron microscopy was used to visualize the fine structure of the lateral line nerve and was performed as described by others (Czopka and Lyons, 2011). Briefly, 4 dpf larvae were fixed with 2% glutaraldehyde, 4% paraformaldehyde and 0.1 M sodium

cacodylate buffer, pH 7.4. Tissue processing was accelerated by microwaving using a Panasonic Inverter NN-SD466M microwave. Secondary fixation was performed with 2% OsO₄, 0.1 M sodium cacodylate and 0.1 M imidazole, pH 7.5, then specimens stained with saturated uranyl acetate. Specimens were embedded in Embed 812 resin (Electron Microscopy Services) and ultrathin sections cut using a Leica EM UC6 ultramicrotome. Electron micrographs were collected using a FEI Tecnai G2 Spirit BioTwin TEM with Gatan MS600CW digital camera in the Department of Biomedical Science EM Suite at the University of Sheffield.

Poly(A)+ RNA hybridization

Paraffin-embedded embryos were transversely dissected in 5µm sections using a microtome (Microm, Germany), floated on warm DEPC-treated water, then collected on charged slides and incubated at 42 °C overnight. The sections were then incubated at 60 °C for thirty minutes followed by dewaxing in xylene for five minutes. Samples were then washed twice in 100% ethanol and in 95% ethanol for five minutes each. They were digested at room temperature with 12.5 µg/ml pepsin (Sigma) in 0.2 M HCl for 20 minutes, before being fixed in ice-cold 4% PFA in PBS for 5 minutes. Excess PFA was removed and the slides were then placed in water for 5 minutes. Samples were transferred to 95% ethanol and then air-dried for 5 minutes. Samples were pre-hybridized in hybridization buffer (20% formamide, 2x SSC, 10% dextran sulphate, 1% BSA, 20 µg/ml salmon sperm DNA and 0.3 µg/ml yeast tRNA) at 42 °C for 30 minutes. They were rinsed in 4x SSC and probed with 1 µg/ml of 5'-Cy3-conjugated oligo(dT) (Eurofins, Germany) in hybridization buffer at 42 °C overnight. They were then washed sequentially in 2x, 1x and 0.1x SSC, rinsed in water and mounted in a hard set mounting medium with DAPI (Vector Laboratories, USA). Samples were imaged using confocal microscopy.

RESULTS

***gle1*^{hi4161aTg/hi4161aTg} mutants exhibit severe developmental defects**

A zebrafish insertional mutant (*gle1*^{hi4161aTg/+}) was generated in a screen for genes essential for zebrafish development (Amsterdam et al., 2004). The retroviral introduced insertion is within the first exon of the *gle1* gene (Fig.1A), thereby generating a non-functional allele. Carrier embryos were obtained from ZIRC (Oregon, USA) and out-crossed with the wild type TL line. To analyze survival, *gle1* mutation carriers were mated, embryos collected and observed at 12-hour intervals. Mutant embryos (henceforth referred to as *gle1*^{-/-}) were initially indiscernible from siblings, but could be distinguished on the basis of a smaller head and eyes from 2 days post-fertilization (dpf). The phenotype of the mutants progressively degenerated with median survival of 6 dpf (Fig.1B). Dead mutant embryos were selected and genotyped to confirm that they were homozygous for the mutant allele. At 4-5 dpf mutant embryos showed pleiotropic phenotypes including small eyes, the lack of a normal lower jaw, pericardial edema and failure to inflate the swim bladder (Fig. 1C). The *gle1* gene is ubiquitously expressed through 24 hpf (Jao et al., 2012), whereas at later stages (48-72 hpf) expression is prominent in tissues that show morphological defects in *gle1*^{-/-} embryos such as the eyes, pectoral fin buds, intestine and pharyngeal arches. In agreement with Mendelian ratios for recessive genes, 24.8% of embryos displayed the mutant phenotype ($n_{\text{mutant}}=169$, $n_{\text{sibling}}=512$). The motility of embryos was analyzed at 4, 5 and 6 dpf by recording the locomotion activity of mutants and siblings over a 2-hour period. A significant reduction in locomotion of the mutants compared to sibling embryos was observed ($p<0.002$ at 4 dpf and $p<0.0001$ at 5 and 6 dpf) (Fig. 1D).

***gle1*^{-/-} mutants show pronounced cell death in the eye and central nervous system**

To determine the effect of *gle1* loss on cell survival, Terminal deoxynucleotidyl transferase dUTP nick end labeling (TUNEL) was used to assess cell death in *gle1*^{-/-} mutant embryos. Very few TUNEL-positive cells were observed in the central nervous system (CNS) or body

of the siblings (Fig. 2A), whereas mutants exhibited considerable levels of cell death in the head and body at 3 dpf (Fig. 2B). Particularly high levels of TUNEL-labeling were observed in the eyes of the mutants (Fig. 2B). Significant TUNEL-labeling was also observed in the spinal cord of *gle1*^{-/-} mutants compared with controls at 3 dpf (Fig. 2C). The mutant embryos analysed in this experiment carried a *Tg(mnx1:GFP)* transgene (commonly referred to as HB9:GFP) for motor neuron identification. This demonstrated that the majority of the TUNEL-positive cells were not GFP-positive. Cell count revealed that around 2% of GFP-positive cells were TUNEL-positive, indicating that only a small proportion of apoptotic cells in the spinal cord were motor neurons (Fig. 2C). Hematoxylin and eosin staining revealed the presence of condensed dead cells in the eyes of *gle1*^{-/-} mutants at 3 dpf, most notably in the pigmented epithelium and inner nuclear layer (Fig. 2D). This contrasted with sibling embryos where a normal retinal structure was observed (Fig. 2E).

Oligodendrocyte development in *gle1*^{-/-} embryos

RNA expression profiling of spinal cord from LCCS1 fetuses has indicated that oligodendrocyte dysfunction may be a factor in disease pathogenesis (Pakkasjarvi et al., 2006). However, this has never been established in an animal model of LCCS1. We therefore investigated oligodendrocyte development with whole-mount RNA *in situ* hybridization using antisense riboprobes for *oligodendrocyte lineage transcription factor 2* (*olig2*), which is expressed by oligodendrocyte precursor cells (OPCs), and *myelin basic protein* (*mbp*), which serves as a marker for myelinating oligodendrocytes and Schwann cells. Analysis of embryos fixed at 51 hours post-fertilization (hpf) revealed that *gle1*^{-/-} mutants (n=35) had a near total loss of *olig2* expression in cerebellar eurydendroid neurons compared to siblings (n=99; Fig. 3A and 3B). This loss of cerebellar *olig2* expression in *gle1*^{-/-} mutants may be correlated with prominent *gle1* expression observed in the cerebellum of wild type embryos around 48 hpf (Jao et al., 2012). However, the overall pattern of *olig2* expression throughout the rest of brain was relatively normal in *gle1*^{-/-} mutants (Fig. 3C)

compared to siblings (Fig. 3D). A reduction in the number of cells scattered throughout the hindbrain was observed in *gle1*^{-/-} mutants compared to controls, which might represent an impairment of OPC migration into the mantle region or a slight developmental delay in the mutant embryos. Analysis of *mbp* expression at 4 dpf showed strong *mbp* expression on both sides of the midline of the hindbrain in both *gle1*^{-/-} mutants and controls (Figs. 3E and F arrowheads), suggesting that oligodendrocytes are able to develop in the absence of *Gle1* function. However, while the pattern of *mbp* expression demonstrated that oligodendrocyte development appeared relatively normal in the hindbrain of *gle1*^{-/-} mutants, the same analysis revealed a striking loss of *mbp* expression in the anterior lateral line (ALLn) and posterior lateral line (PLLn) nerves (arrows in Fig. 3F), suggesting a potential defect in Schwann cell development in *gle1*^{-/-} mutants.

Defective Schwann cell development in *gle1*^{-/-} embryos

Whole mount *in situ* hybridization for *mbp* mRNA at 4-5 dpf revealed prominent expression along most or the full length of the PLLn in control embryos (n=136; arrows in Fig 4B), whereas in *gle1*^{-/-} mutant embryos (n=45), *mbp* expression along the PLLn was restricted to the most anterior somites (arrow in Fig. 4A). The expression of *mbp* mRNA was similarly restricted to the anterior portion of the PLLn at 6 dpf in *gle1*^{-/-} mutant embryos (n=24; not shown). A similar striking loss of *mbp* expression was apparent in the ALLn, with minimal *mbp* expression observed in *gle1*^{-/-} mutants (arrowheads in Fig. 4A and B). Staining of axons with an anti-acetylated tubulin antibody demonstrated that the PLLn extended the full length of the embryo in *gle1*^{-/-} mutants (n=25) and siblings (n=108; arrows in Fig. 4C, D). It is therefore unlikely that the loss of *mbp* expression in *gle1*^{-/-} mutants is due to axon outgrowth defects in the lateral line, and more likely represents a defect in Schwann cell development.

Previous studies have shown that the myelination defects in *erbb3* mutant zebrafish are due to impaired migration and proliferation of Schwann cell precursors (Lyons et al., 2005). Given that mutations in *GLE1* and *ERBB3* both cause LCCS in humans, we reasoned

that *gle1*^{-/-} mutants may show similar defects to those seen in *erbb3* mutants. To investigate this, we analyzed *sox10* expression (a marker for Schwann cell precursors) in *gle1*^{-/-} mutants (n=18) and siblings (n=70). Expression of *sox10* in Schwann cell precursors was seen continuously along the length of the PLLn in control embryos (Fig. 4F), whereas in *gle1*^{-/-} mutants, *sox10* expression was weaker and interrupted along the PLLn, implying reduced numbers of Schwann cell precursors along the PLLn (Fig. 4E). This differs from what is seen in *erbb3* mutants where *sox10* expression is practically absent from the PLLn (Lyons et al., 2005). Analysis of *krox20* expression (a marker for Schwann cells committed to myelination) similarly demonstrated that *krox20* expression was present along the PLLn in *gle1*^{-/-} mutants (Fig. 4G; n=31), but was less intense compared with controls (Fig. 4H; n=131).

In order to ascertain whether the apparent reduction in the number of Schwann cell precursors along the PLLn was due to a proliferation defect we crossed *gle1*^{hi4161Tg/+} carriers with *Tg(sox10:mRFP)* fish to generate double transgenic carriers. These fish were in-crossed and offspring labelled with the thymidine analog 5-ethynyl-2'-deoxyuridine (EdU) via direct injection into the yolk mass at 52 hpf. Reduced EdU incorporation was apparent in multiple tissues throughout mutant embryos and a significant reduction in the number of EdU-labelled mRFP⁺ Schwann cell precursors was observed along the PLLn in homozygous *gle1*^{-/-} mutants (1.8 ± 0.3 EdU-positive cells/100 μm along the PLLn in mutants compared with 4.0 ± 0.4 cells/100 μm in siblings; P=0.003, Mann-Whitney U test), demonstrating that Gle1 function is essential for normal proliferation of Schwann cell precursors at this stage (Fig. 5).

To determine the effect of loss of Gle1 function on myelination of the PLLn, structural analysis using transmission electron microscopy (TEM) was undertaken. At 4 dpf, loosely wrapped myelin membranes (typically 3-4 per axon) were apparent on nearly all PLLn axons in control sibling embryos (Fig. 6A). In stark contrast, PLLn axons in *gle1*^{-/-} mutant embryos were practically devoid of myelin membrane (Fig. 6B). Quantification of the number of wraps of myelin membrane per axon is shown in Fig. 6C. Additionally, the mean axon diameter in

gle1^{-/-} mutant embryos was significantly smaller ($0.5 \pm 0.04 \mu\text{m}$ in mutants compared with $1.42 \pm 0.07 \mu\text{m}$ in control embryos; Fig. 6D). Gle1 function therefore appears to be essential for the proliferation and differentiation of Schwann cell precursors into myelinating Schwann cells.

***gle1*^{-/-} mutants show poly(A)⁺ RNA export defects and nuclear mRNA accumulation**

Previous studies have demonstrated that Gle1 is involved in poly(A)⁺ RNA export from the nucleus (Murphy and Wentz, 1996, Alcazar-Roman et al., 2006). Based on these findings, we reasoned that *gle1*^{-/-} mutants would show nuclear mRNA accumulation. Fluorescent *in situ* hybridization using 5'-Cy3-conjugated oligo(dT), which hybridizes to the poly(A) tail of mRNA confirmed this. Confocal imaging revealed that *gle1*^{-/-} mutants showed intense Cy3 nuclear staining, suggesting accumulation of poly(A)⁺ RNA in the nucleus (Fig. 7D-F), whereas siblings showed diffuse staining, indicating a more even distribution throughout the nucleus and cytoplasm (Fig. 7A-C). Nuclear accumulation of poly(A)⁺ RNA was seen in sections throughout the head, eye and spinal cord (not shown).

DISCUSSION

LCCS1 is an autosomal recessive disorder caused by mutation of *GLE1* which is characterized by total immobility of the fetus and presents with multiple joint contractures, facial abnormalities, severe muscle atrophy and degeneration of the anterior horn of the spinal cord. In keeping with a multi-systemic disorder, homozygous *gle1*^{-/-} mutant zebrafish embryos show prominent ocular and craniofacial abnormalities, reduced motility and increased CNS apoptosis. Mutants can be identified from 2 dpf based on the small eye phenotype and survive on average to 6 dpf, with maximal survival of around 9 dpf. While LCCS1 patients show marked loss of motor neurons in the anterior horn, *gle1*^{-/-} zebrafish mutants show a relatively minor decrease in motor neuron numbers (Jao et al., 2012) in

comparison with other phenotypes in the same embryos, suggesting that other factors may contribute to motor neuron loss in LCCS1 cases. We herein demonstrate a critical requirement for normal *gle1* gene function in Schwann cell development, thereby suggesting that myelination defects may be an important factor in LCCS1. This adds to the significance of recent studies demonstrating roles for other LCCS genes in peripheral myelination and suggests that Schwann cell deficits may be a common feature of this syndrome.

It is apparent that a number of the LCCS genes involved in PNS myelination have different roles in Schwann cell development and function. In the zebrafish embryo, *erbb3* has been shown to be specifically required for migration and proliferation of Schwann cell precursors (Lyons et al., 2005). CNTNAP1 on the other hand, mediates axon-glia contacts in paranodal regions and its loss affects saltatory nerve conduction (Bhat et al., 2001). Whole mount *in situ* hybridization for *sox10* and *krox20* demonstrated that Schwann cell precursors initially populate the PLLn in *gle1*^{-/-} mutants (Fig. 4). However these cells show reduced proliferation (Fig. 5) and fail to differentiate normally on the basis of greatly reduced *mbp* expression (Fig. 4) and the failure to envelop axons with myelinating membranes (Fig. 6). This phenotype resembles that observed in *adcy6* morpholino mutants (morphants), where greatly reduced *mbp* expression was observed along the PLLn in spite of apparently normal expression of markers for PLLn axons and Schwann cell precursors (Laquérière et al., 2014).

In agreement with previous studies in yeast and cultured human cells (Watkins et al., 1998, Kendirgi et al., 2003), our study revealed a defect in mRNA export in *gle1*^{-/-} mutants as evidenced by poly(A)⁺ RNA accumulation in the nucleus. One question that arises is whether the observed Schwann cell defects in *gle1*^{-/-} mutant embryos are a direct consequence of impaired mRNA export? The importance of *mbp* mRNA transport from the cell body to processes during oligodendrocyte development has been well characterized (Lyons et al., 2009). A similar requirement for *mbp* mRNA transport during Schwann cell development has not been documented, but RNA transport and local translation have been reported in

Schwann cells (Gould and Mattingly, 1990), so one hypothesis is that normal Gle1 function is required for nuclear export and/or transport of *mbp* mRNA in differentiating Schwann cells. Alternatively, the failure to myelinate PLLn axons may be a consequence of reduced axon calibre (Michailov et al., 2004).

Genes involved in different aspects of RNA biology have been linked to a number of motor neuron diseases. These include *SMN* in SMA, *GLE1* in LCCS1 and *TARDBP*, *FUS* and *GLE1* in ALS (Lefebvre et al., 1995, Sreedharan et al., 2008, Nousiainen et al., 2008, Vance et al., 2009, Folkmann et al., 2013). Interestingly, all have been implicated in multiple aspects of RNA metabolism. *SMN* is associated with assembly of ribonucleoprotein (RNP) complexes, splicing and axonal mRNA transport; *GLE1* is involved in the nuclear export of mRNA as well as translation initiation and termination, while *TARDBP* and *FUS* have roles in the regulation of gene expression, splicing, formation of RNP complexes and microRNA processing. The role that these proteins play in RNA processing in relation to motor neuron biology has become an intensive area of research. The data reported here show a novel requirement for the RNA export mediator Gle1 in Schwann cell development, suggesting that RNA metabolism in glial cells may also be an important factor in motor neuron survival. In support of this notion, Schwann cell defects have recently been reported in two forms of SMA (Hunter et al., 2014, Jędrzejowska et al., 2014). Peripheral nerve myelination defects were shown in two SMA mouse models and Schwann cells isolated from SMA mice failed to express key myelin proteins when differentiated (Hunter et al., 2014). This suggests that Schwann cell defects may be a common feature of fetal/infantile motor neuron diseases. Modeling in zebrafish therefore allows new insights into fundamental biological mechanisms of motor neuron degeneration linked to RNA processing defects and has the potential to identify novel therapeutic targets for motor neuron diseases.

Acknowledgements

MA is supported by ERC Advanced Investigator Award (294745) and MRC DPFS Award (129016). We would like to thank Dr. David Lyons, Marja Karttunen (both University of Edinburgh) and Chris Hill (Department of Biomedical Science EM Suite, University of Sheffield) for assistance with TEM, Dr. Vincent Cunliffe for providing the *Tg(mnx1:gfp)* line and Dr. Sarah Baxendale for assistance using the Viewpoint system. We are grateful to Claire Allen, Lisa van Hateren, Susanne Surfleet, Matthew Green and Michael Thomas for fish care. ZIRC is supported by grant P40 RR012546 from the NIH-NCRR. Antibodies obtained from DSHB were developed under the auspices of the NICHD and maintained by The University of Iowa, Department of Biology, Iowa City, U.S.A. Zebrafish facilities were supported through MRC awards G0400100 and G0700091.

REFERENCES

- Alcazar-Roman AR, Tran EJ, Guo S, Wente SR (2006) Inositol hexakisphosphate and Gle1 activate the DEAD-box protein Dbp5 for nuclear mRNA export. *Nat Cell Biol* 8:711-716.
- Amsterdam A, Nissen RM, Sun Z, Swindell EC, Farrington S, Hopkins N (2004) Identification of 315 genes essential for early zebrafish development. *Proc Natl Acad Sci U S A* 101:12792-12797.
- Bhat MA, Rios JC, Lu Y, Garcia-Fresco GP, Ching W, St Martin M, Li J, Einheber S, Chesler M, Rosenbluth J, Salzer JL, Bellen HJ (2001) Axon-glia interactions and the domain organization of myelinated axons requires neurexin IV/Caspr/Paranodin. *Neuron* 30:369-383.
- Bolger TA, Folkmann AW, Tran EJ, Wente SR (2008) The mRNA export factor Gle1 and inositol hexakisphosphate regulate distinct stages of translation. *Cell* 2008 Aug 22;134(4): 134:624-633.
- Boon KL, Xiao S, McWhorter ML, Donn T, Wolf-Saxon E, Bohnsack MT, Moens CB, Beattie CE (2009) Zebrafish survival motor neuron mutants exhibit presynaptic neuromuscular junction defects. *Human Molecular Genetics* 18:3615-3625.
- Czopka T, Lyons DA (2011) Dissecting mechanisms of myelinated axon formation using zebrafish. *Methods Cell Biol* 105:25-62.
- Folkmann AW, Collier SE, Zhan X, Aditi OMD, SR. W (2013) Gle1 functions during mRNA export in an oligomeric complex that is altered in human disease. *Cell* 155:582-593.
- Gatto CL, Walker BJ, Lambert S (2007) Asymmetric ERM activation at the Schwann cell process tip is required in axon-associated motility. *J Cell Physiol* 210:122-132.
- Gould RM, Mattingly G (1990) Regional localization of RNA and protein metabolism in Schwann cells in vivo. *J Neurocytol* 19:285-301.

- Hodge CA, Tran EJ, Noble KN, Alcazar-Roman AR, Ben-Yishay R, Scarcelli JJ, Folkmann AW, Shav-Tal Y, Wentz SR, Cole CN (2011) The Dbp5 cycle at the nuclear pore complex during mRNA export I: dbp5 mutants with defects in RNA binding and ATP hydrolysis define key steps for Nup159 and Gle1. *Genes Dev* 25:1052–1064.
- Hunter G, Aghamaleky Sarvestany A, Roche SL, Symes RC, Gillingwater TH (2014) SMN-dependent intrinsic defects in Schwann cells in mouse models of spinal muscular atrophy. *Hum Mol Genet* 23:2235-2250.
- Ibrahim F, Nakaya T, Mourelatos Z (2012) RNA dysregulation in diseases of motor neurons. *Annu Rev Pathol* 7:323-352.
- Jao LE, Appel B, Wentz SR (2012) A zebrafish model of lethal congenital contracture syndrome 1 reveals Gle1 function in spinal neural precursor survival and motor axon arborization. *Development* 139:1316-1326.
- Jędrzejowska M, Gos M, Zimowski JG, Kostera-Pruszczyk A, Ryniewicz B, Hausmanowa-Petrusewicz I (2014) Novel point mutations in survival motor neuron 1 gene expand the spectrum of phenotypes observed in spinal muscular atrophy patients. *Neuromuscul Disord* 24:617-623.
- Kabashi E, Champagne N, Brustein E, Drapeau P (2010) In the swim of things: recent insights to neurogenetic disorders from zebrafish. *Trends Genet* 26:373-381.
- Kaneb HM, Folkmann AW, Belzil VV, Jao LE, Leblond CS, Girard SL, Daoud H, Noreau A, Rochefort D, Hince P, Szuto A, Levert A, Vidal S, André-Guimont C, Camu W, Bouchard JP, Dupré N, Rouleau GA, Wentz SR, Dion PA (2015) Deleterious mutations in the essential mRNA metabolism factor, hGle1, in amyotrophic lateral sclerosis. *Hum Mol Genet* 24:1363-1373.
- Kendirgi F, Barry DM, Griffis ER, Powers MA, Wentz SR (2003) An essential role for hGle1 nucleocytoplasmic shuttling in mRNA export. *J Cell Biol* 160:1029-1040.

- Kendirgi F, Rexer DJ, Alcazar-Roman AR, Onishko HM, Wentz SR (2005) Interaction between the shuttling mRNA export factor Gle1 and the nucleoporin hCG1: a conserved mechanism in the export of Hsp70 mRNA. *Mol Biol Cell* 16:4304-4315.
- Koutsopoulos OS, Kretz C, Weller CM, Roux A, Mojzisova H, Böhm J, Koch C, Toussaint A, Heckel E, Stemkens D, Ter Horst SA, Thibault C, Koch M, Mehdi SQ, Bijlsma EK, Mandel JL, Vermot J, Laporte J (2013) Dynamin 2 homozygous mutation in humans with a lethal congenital syndrome. *Eur J Hum Genet* 21:637-642.
- Kucenas S, Takada N, Park HC, Woodruff E, Broadie K, B. A (2008) CNS-derived glia ensheath peripheral nerves and mediate motor root development. *Nat Neurosci* 11:143-151.
- Laquérière A, Maluenda J, Camus A, Fontenas L, Dieterich K, Nolent F, Zhou J, Monnier N, Latour P, Gentil D (2014) Mutations in CNTNAP1 and ADCY6 are responsible for severe arthrogryposis multiplex congenita with axoglial defects. *Hum Mol Genet* 23:2279-2289.
- Lefebvre S, Burglen L, Reboullet S, Clermont O, Burllet P, Viollet L, Benichou B, Cruaud C, Millasseau P, Zeviani M (1995) Identification and characterization of a spinal muscular atrophy-determining gene. *Cell* 80:155-165.
- Lyons DA, Naylor SG, Scholze A, Talbot WS (2009) Kif1b is essential for mRNA localization in oligodendrocytes and development of myelinated axons. *Nat Genet* 41:854-858.
- Lyons DA, Pogoda HM, Voas MG, Woods IG, Diamond B, Nix R, Arana N, Jacobs J, Talbot WS (2005) *erbb3* and *erbb2* are essential for schwann cell migration and myelination in zebrafish. *Curr Biol* 15:513-524.
- Michailov GV, Sereda MW, Brinkmann BG, Fischer TM, Haug B, Birchmeier C, Role L, Lai C, Schwab MH, Nave KA (2004) Axonal neuregulin-1 regulates myelin sheath thickness. *Science* 304:700-703. .
- Murphy R, Wentz SR (1996) An RNA-export mediator with an essential nuclear export signal. *Nature* 383:357-360.

- Narkis G, Ofir R, Landau D, Manor E, Volokita M, Hershkowitz R, Elbedour K, Birk OS (2007a) Lethal contractural syndrome type 3 (LCCS3) is caused by a mutation in PIP5K1C, which encodes PIPKI gamma of the phosphatidylinositol pathway. *Am J Hum Genet* 81:530-539.
- Narkis G, Ofir R, Manor E, Landau D, Elbedour K, Birk OS (2007b) Lethal congenital contractural syndrome type 2 (LCCS2) is caused by a mutation in ERBB3 (Her3), a modulator of the phosphatidylinositol-3-kinase/Akt pathway. *Am J Hum Genet* 81:589-595.
- Noble KN, Tran EJ, Alcazar-Roman AR, Hodge CA, Cole CN, R. WS (2011) The Dbp5 cycle at the nuclear pore complex during mRNA export II: nucleotide cycling and mRNP remodeling by Dbp5 are controlled by Nup159 and Gle1. *Genes Dev* 25:1065–1077.
- Nousiainen HO, Kestilä M, Pakkasjärvi N, Honkala H, Kuure S, Tallila J, Vuopala K, Ignatius J, Herva R, Peltonen L (2008) Mutations in mRNA export mediator GLE1 result in a fetal motoneuron disease. *Nat Genet* 40:155-157.
- Pakkasjarvi N, Ritvanen A, Herva R, Peltonen L, Kestila M, Ignatius J (2006) Lethal congenital contracture syndrome (LCCS) and other lethal arthrogryposes in Finland-an epidemiological study. *Am J Med Genet A* 140:1834–1839.
- Ramesh T, Lyon AN, Pineda RH, Wang CP, Janssen PML, Canan BD, Burghes AHM, Beattie CE (2010) A genetic model of amyotrophic lateral sclerosis in zebrafish displays phenotypic hallmarks of motoneuron disease. *Disease Models & Mechanisms* 3:652-662.
- Rayala HJ, Kendirgi F, Barry DM, Majerus PW, Wente SR (2004) The mRNA export factor human Gle1 interacts with the nuclear pore complex protein Nup155. *Mol Cell Proteomics* 3:145-155.
- Riethmacher D, Sonnenberg-Riethmacher E, Brinkmann V, Yamaai T, Lewin GR, Birchmeier C (1997) Severe neuropathies in mice with targeted mutations in the ErbB3 receptor. *Nature* 389:725-730.

- Sidiropoulos PN, Mieke M, Bock T, Tinelli E, Oertli CI, Kuner R, Meijer D, Wollscheid B, Niemann A, Suter U (2012) Dynamin 2 mutations in Charcot-Marie-Tooth neuropathy highlight the importance of clathrin-mediated endocytosis in myelination. *2012 Brain* 135:1395-1411.
- Sreedharan J, Blair IP, Tripathi VB, Hu X, Vance C, Rogelj B, Ackerley S, Durnall JC, Williams KL, Buratti E, Baralle F, de Belleruche J, Mitchell JD, Leigh PN, Al-Chalabi A, Miller CC, Nicholson G, Shaw CE (2008) TDP-43 mutations in familial and sporadic amyotrophic lateral sclerosis. *Science* 319:1668-1672.
- Tran EJ, Zhou Y, Corbett AH, Wentz SR (2007) The DEAD-box protein Dbp5 controls mRNA export by triggering specific RNA:protein remodeling events. *Mol Cell* 28:850–859
- Vance C, Rogelj B, Hortobágyi T, De Vos K, et al. (2009) Mutations in FUS, an RNA Processing Protein, Cause Familial Amyotrophic Lateral Sclerosis Type 6. *Science* 323:1208.
- Watkins JL, Murphy R, Emtage JL, R. WS (1998) The human homologue of *Saccharomyces cerevisiae* Gle1p is required for poly(A)⁺ RNA export. *Proc Natl Acad Sci USA* 95:6779–6784.
- Xi Y, Noble S, Ekker M (2011) Modeling neurodegeneration in zebrafish. *Curr Neurol Neurosci Rep* 11:274-282.

Legends to Figures:

Fig. 1. Homozygous *gle1* insertional mutants show severe developmental defects, reduced motility and premature death. (A) Schematic diagram of *gle1* exon 1 showing the site of retroviral insertion. (B) The survival of *gle1*^{-/-} mutants is greatly reduced compared to their siblings with median survival of 6 dpf and maximal survival around 9 dpf ($p < 0.0001$). (C) Lateral images of sibling (top) and mutant (bottom) embryos at 4.5 dpf demonstrates cardiac edema, failure to inflate the swim bladder, microcephaly, micrognathia, and microphthalmia in *gle1*^{-/-} mutants compared to siblings. Scale bar is 250 μm . (D) The motility of *gle1*^{-/-} mutants was compared to that of their siblings by tracking and recording their movement over a 25-minute dark/5-minute light cycle for 2 hours. The motility of the mutants peaks on day 5 and is significantly less than that of siblings (** $p = 0.002$ on day 4, **** $p < 0.0001$ on days 5 and 6).

Fig. 2. *gle1*^{-/-} mutants exhibit prominent cell death in the eye and spinal cord. (A-B) TUNEL staining of sibling (A) and mutant (B) embryos at 5 dpf demonstrates increased cell death in *gle1*^{-/-} mutants, most notably in the eyes. (C) A lateral image of the spinal cord of a 3 day old *Tg(mnx1:GFP)* expressing *gle1*^{-/-} mutant stained for TUNEL (red) demonstrates that the vast majority of TUNEL-positive cells are GFP-negative and do not co-localise with the motor neurons. (D-E) H&E staining reveals the presence of condensed dead cells in the differentiated retina of *gle1*^{-/-} mutants (D) at 3 dpf which are not seen in sibling controls (E).

Fig. 3. *gle1*^{-/-} mutants lack cerebellar eurydendroid neurons but not oligodendrocyte precursors or oligodendrocytes. Whole-mount *in situ* hybridization for *olig2* expression demonstrated a near total loss of cerebellar eurydendroid neurons in *gle1*^{-/-} mutants (A) which are seen as two semicircular arcs of cells in siblings (arrows in B). Imaging of the same embryos depicted in (A) and (B) at a more ventral plane of focus revealed the presence of *olig2*-positive cells throughout the brain in both *gle1*^{-/-} mutants (C) and siblings

(D), with an apparent reduction in the pepperpot pattern of expression in the mutant hindbrain (arrows). Staining for expression of *mbp* at 4 dpf, a marker for myelinating oligodendrocytes in the hindbrain, showed a similar pattern and intensity of labeling on either side of the midline in mutants (E) and siblings (F). However, a dramatic loss of Schwann cell *mbp* expression in the anterior and posterior lateral line (arrows in F) is apparent in the mutant (E).

Fig. 4. Defective Schwann cell development in *gle1*^{-/-} mutants. (A-F) Embryos lacking *gle1* show greatly reduced expression of genes that mark myelinating Schwann cells along the lateral line nerves. Lateral views of *gle1*^{-/-} mutant (A) and sibling (B) embryos stained for *mbp* expression at 4 dpf by whole mount *in situ* hybridization. Arrows indicate *mbp* expression along the posterior lateral line nerve); arrowheads indicate the position of the anterior lateral line nerve). (C, D) Anti-acetylated tubulin staining of axons in the PLLn (arrowheads) at 4 dpf in *gle1*^{-/-} mutant (C) and sibling (D) control embryos demonstrates that axons form along the length of the PLLn in *gle1*^{-/-} mutant embryos. (E-H) Staining for *sox10* (E, F) and *krox20* (G, H) expression, markers for Schwann cell precursors, in the PLLn at 3-4 dpf (arrows) shows similar but weaker expression in *gle1*^{-/-} mutant embryos (E, G) compared with sibling controls (F, H).

Fig. 5. Mutant *gle1*^{-/-} embryos show reduced proliferation of Schwann cell precursors. Proliferating Schwann cell precursors were identified using EdU-labelling (red) and immunostaining with an anti-DsRed antibody (green) in *Tg(sox10:mRFP)* embryos. EdU-positive cells were readily detected along the PLLn in sibling embryos (A), but sparser and more weakly labelled in *gle1*^{-/-} mutant embryos (B).

Fig. 6. *Gle1* is required for the formation of myelinating Schwann cells. Panels A and B show TEM images of transverse sections through the PLLn. Wild type axons (A) are loosely

wrapped by multiple layers of myelin membrane, whereas mutant axons **(B)** lack myelin; scale bars = 0.5 μm . **(C)** *gle1^{-/-}* mutants show a significant decrease in the number of wraps of myelin membrane per axon compared to siblings (**** $P < 0.0001$; two-tailed, unpaired t-test). **(D)** Mutant axons showed a significant decrease in diameter ($0.5 \pm 0.04 \mu\text{m}$ in mutants compared with $1.42 \pm 0.07 \mu\text{m}$ in control embryos; **** $P < 0.0001$; two-tailed, unpaired t-test).

Fig. 7. Defective mRNA export leads to nuclear accumulation of poly(A)⁺ RNA in *gle1^{-/-}* mutants. Transverse sections of the eye from 3 dpf embryos stained with DAPI (pseudo-colored green) to stain nuclei **(A & D)** and Cy3-labeled oligo(dT) (red; **B & E**). The merged images **(C & F)** demonstrate that *gle1^{-/-}* mutants **(D-F)** show nuclear poly(A)⁺ RNA accumulation compared to sibling embryos **(A-C)** where more diffuse nuclear and cytoplasmic Cy3 fluorescence is observed.

Figure 1

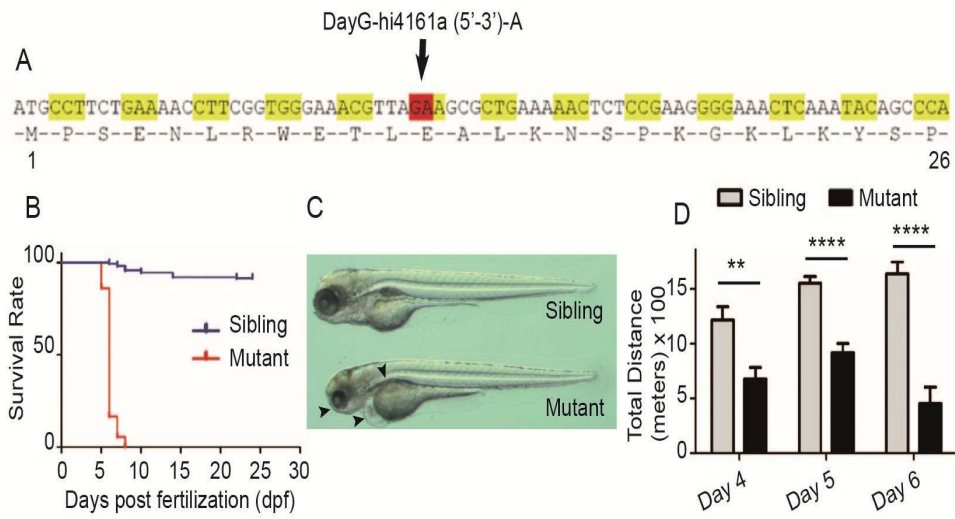


Figure 2

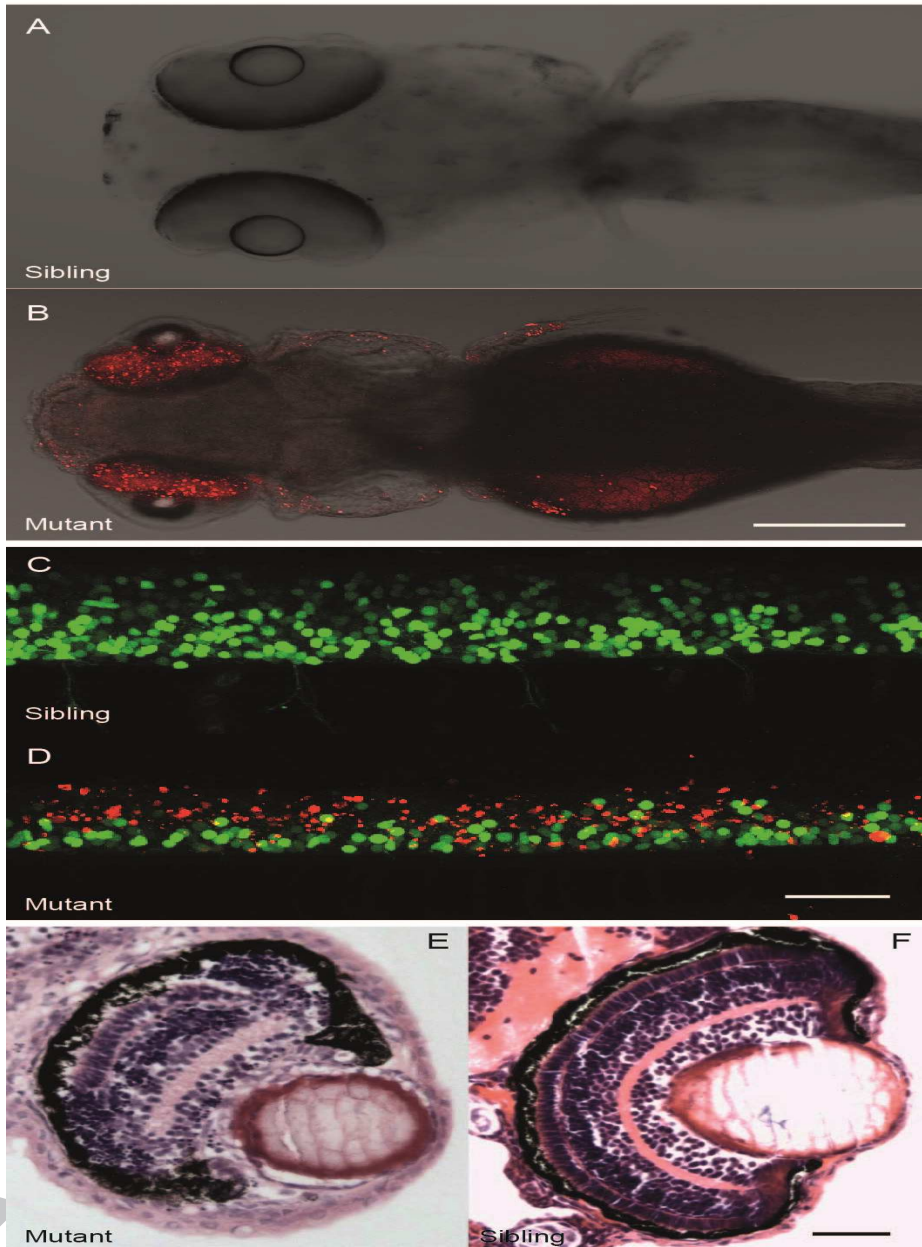


Figure 3

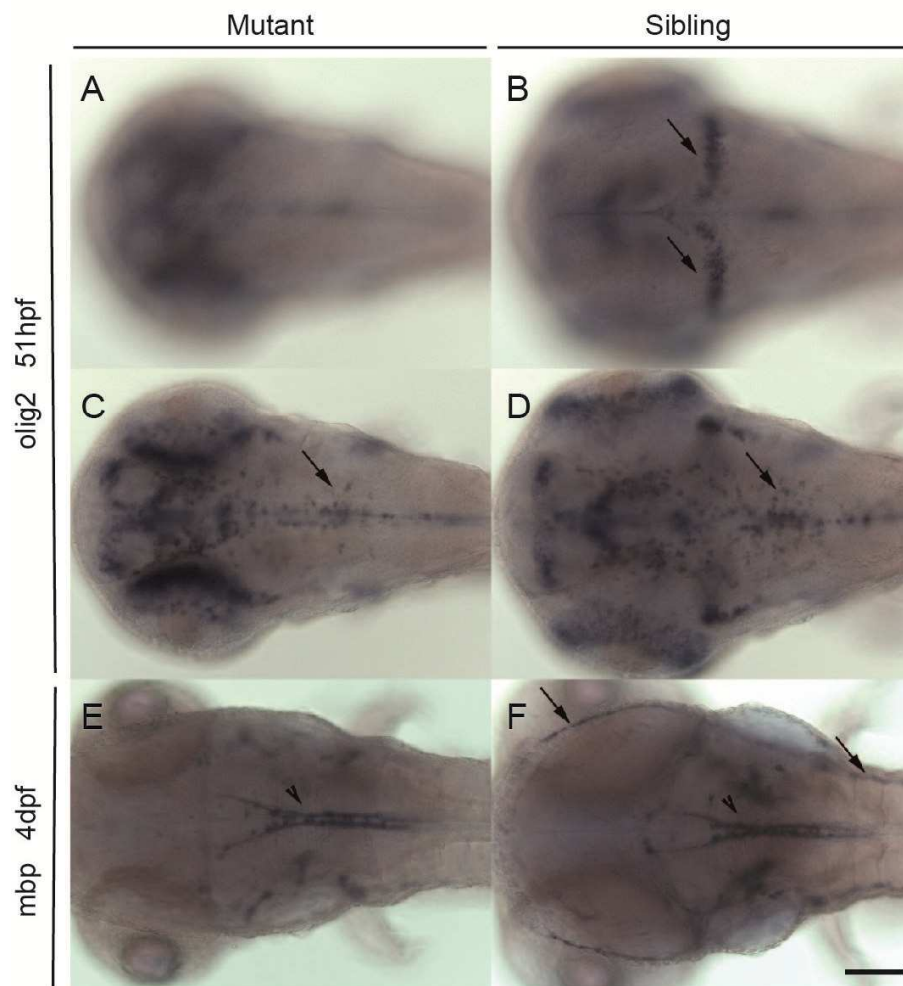


Figure 4

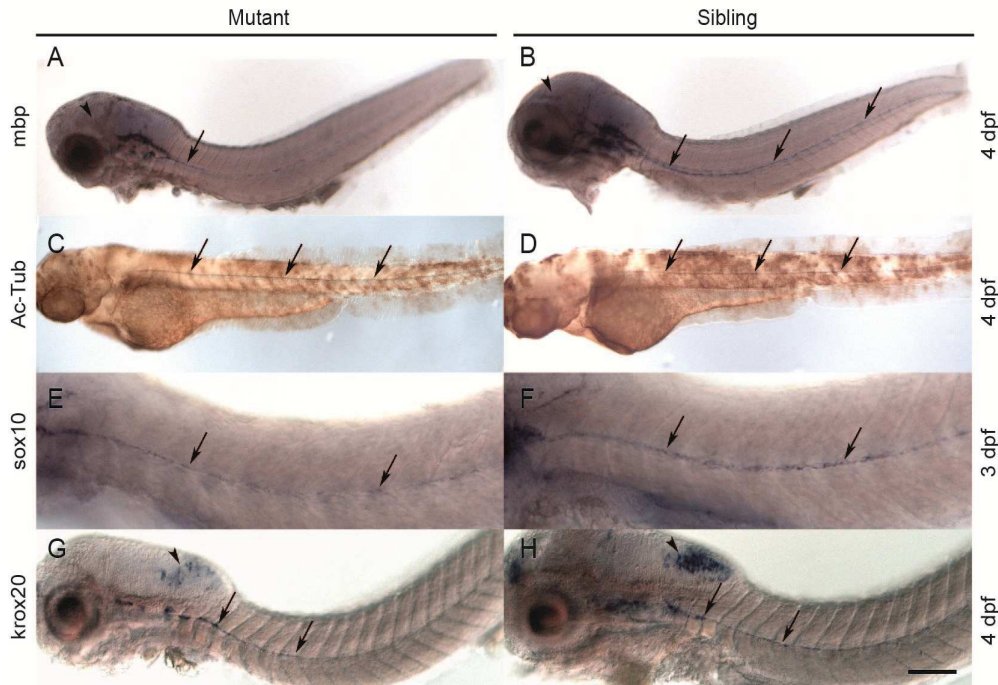


Figure 5

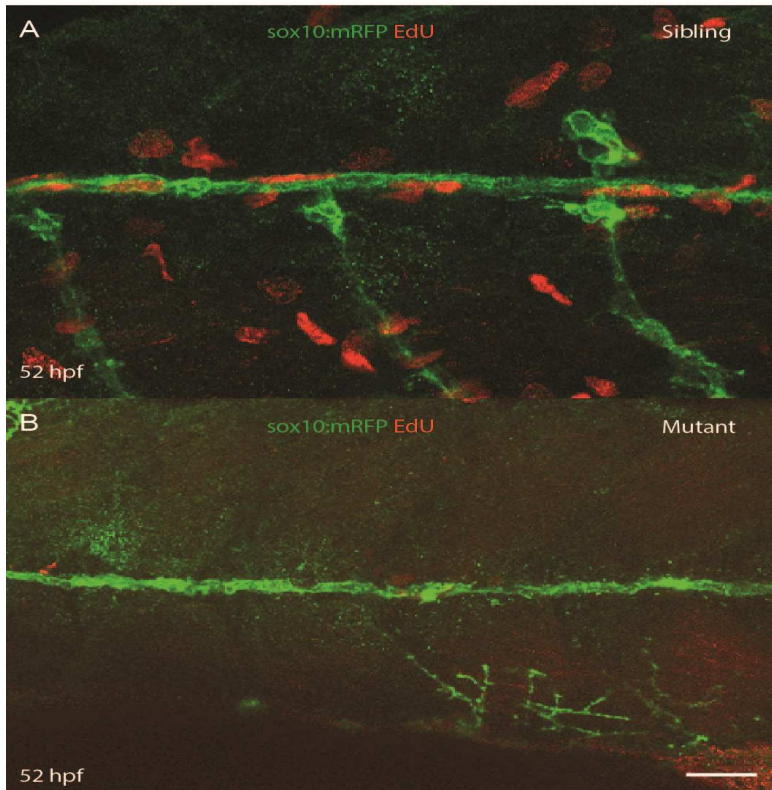


Figure 6

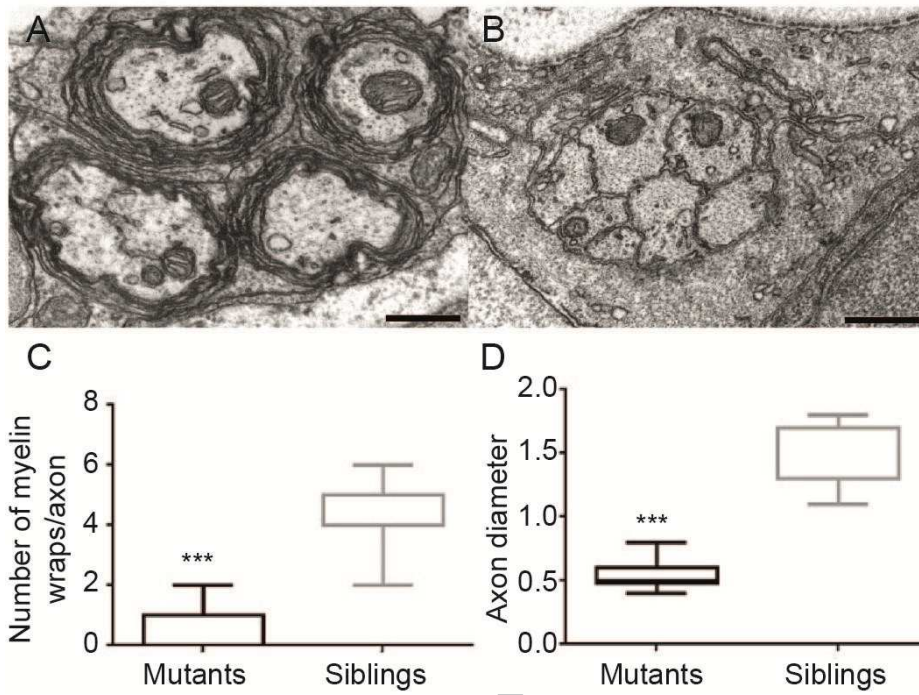
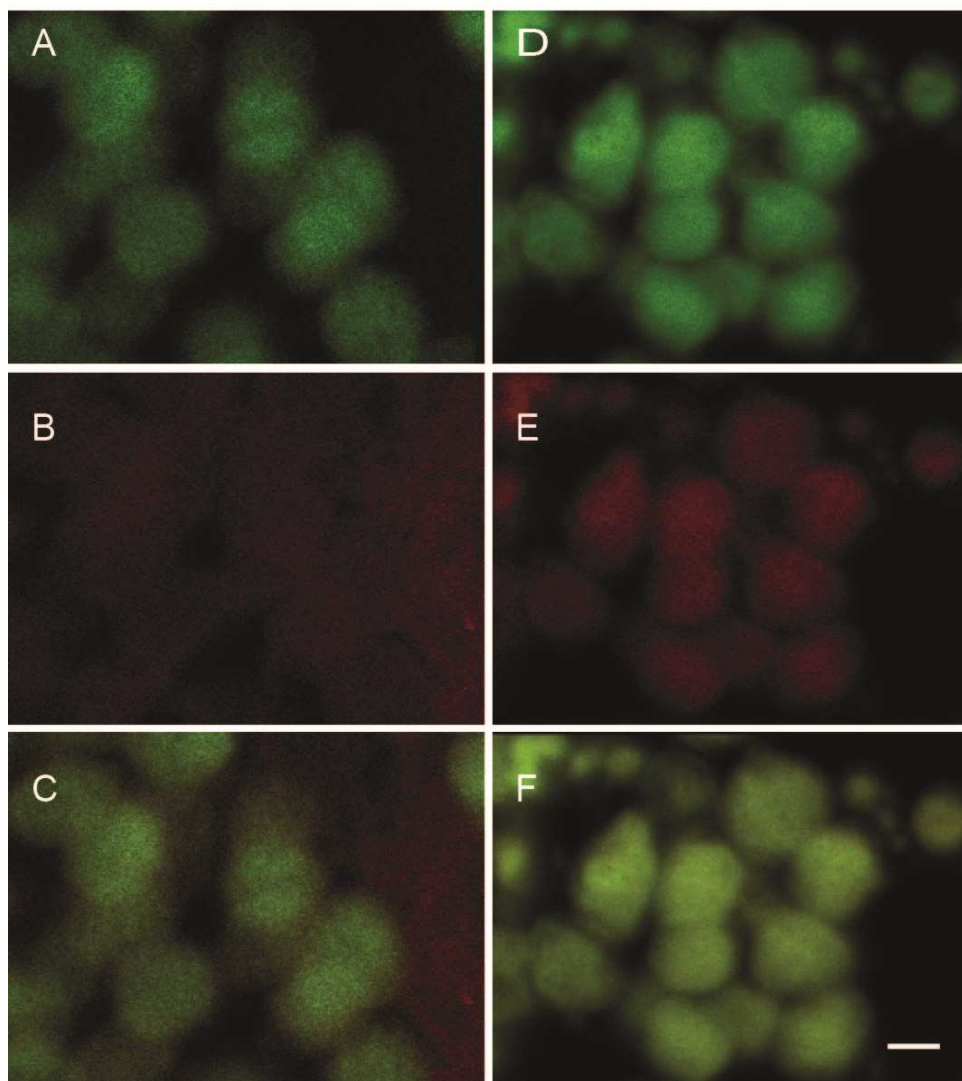


Figure 7



Highlights

- Impact of gle1 depletion on zebrafish development.
- Role of RNA-binding protein gle1 in motor neuron and Schwann cells development
- Schwann cell may have a role in gle1-linked LCCS1 pathology.

ACCEPTED MANUSCRIPT